Heavy ions at the LHC: predictions for net-baryon distributions

Georg Wolschin
Heidelberg University
Institut für Theoretische Physik
Philosophenweg 16
D-69120 Heidelberg

Topics

1. Introduction
2. A QCD-based approach to heavy-ion collisions at the LHC and gluon saturation
3. Net-baryon transverse momentum distributions at RHIC
4. Net-baryon rapidity distributions: Theory vs. data at SPS, RHIC energies; predictions for LHC
5. Conclusion and Outlook

1. Introduction

LHC: Atlas, CMS, LHCb, ALICE

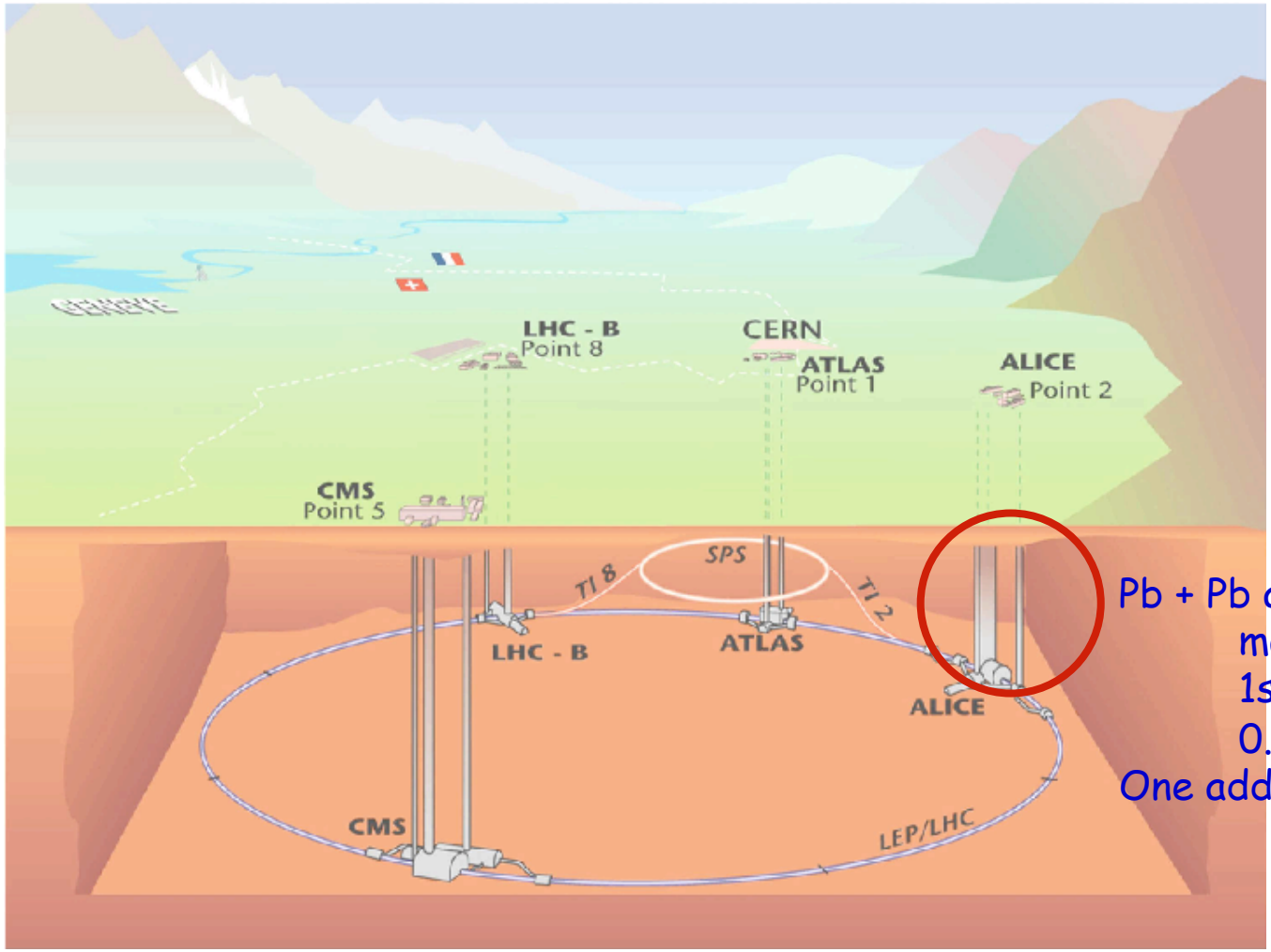

Pb + Pb at LHC:
max. 5.5 TeV/particle pair
1st lead beam Nov 2010 @
0.32 and 2.76 TeV
One add. Run in 2011

LHC: Detectors

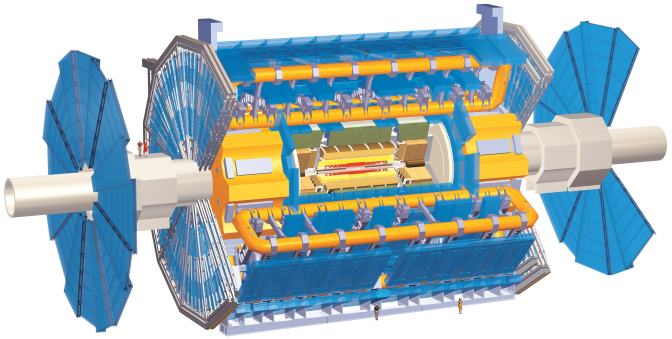

Atlas*

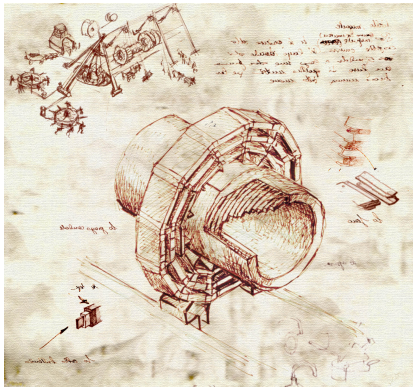

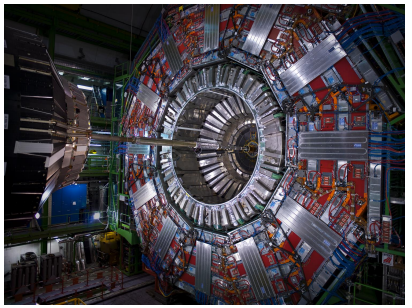

CMS*

da Vinci style

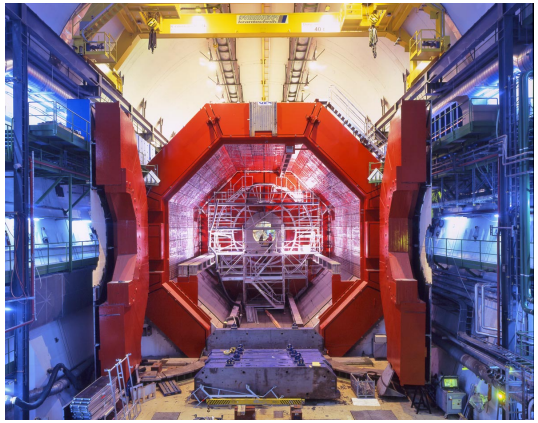

Alice*: L3 magnet

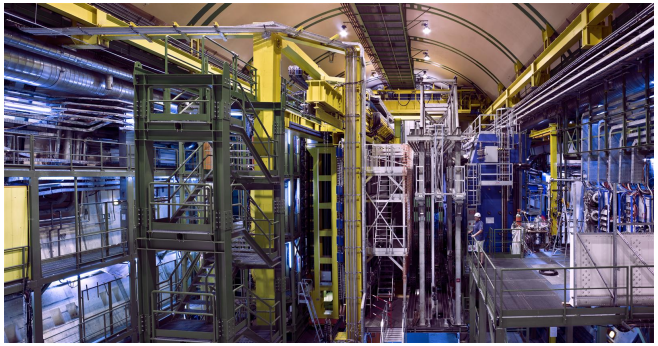

LHCb

* heavy-ion capability

ALICE p+p first results

..... RHIC/Phobos Au + Au

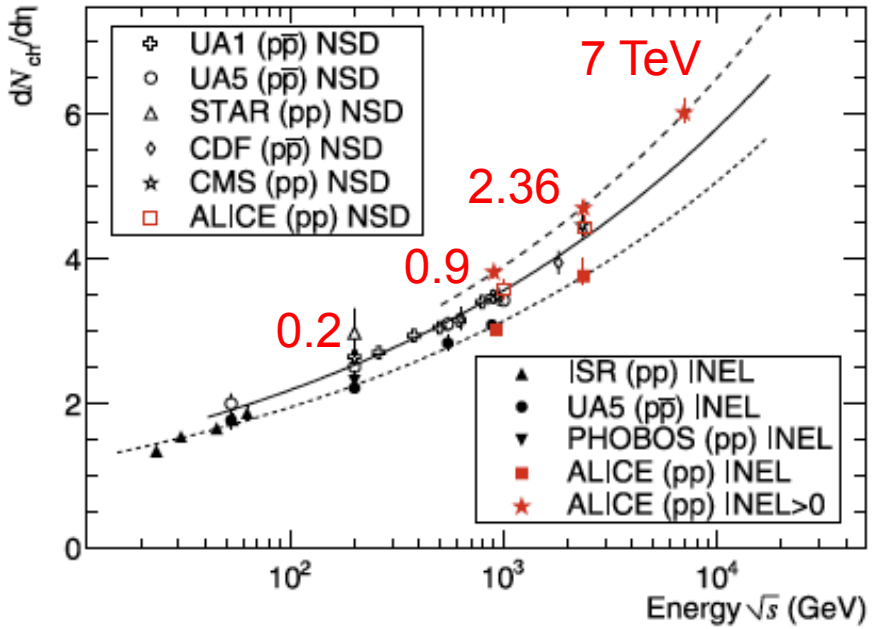

Fig. 2 Charged-particle pseudorapidity density in the central pseudorapidity region $|\eta| < 0.5$ for inelastic and non-single-diffractive collisions [4, 16–25], and in $|\eta| < 1$ for inelastic collisions with at least one charged particle in that region (INEL $> 0_{|\eta|<1}$), as a function of the centre-of-mass energy. The *lines* indicate the fit using a power-law dependence on energy. Note that data points at the same energy have been slightly shifted horizontally for visibility

$$\eta = -\ln|\tan(\theta/2)|$$

ALICE collab., Eur. Phys. J. C 65, 111 (2010); C 68, 345 (2010).

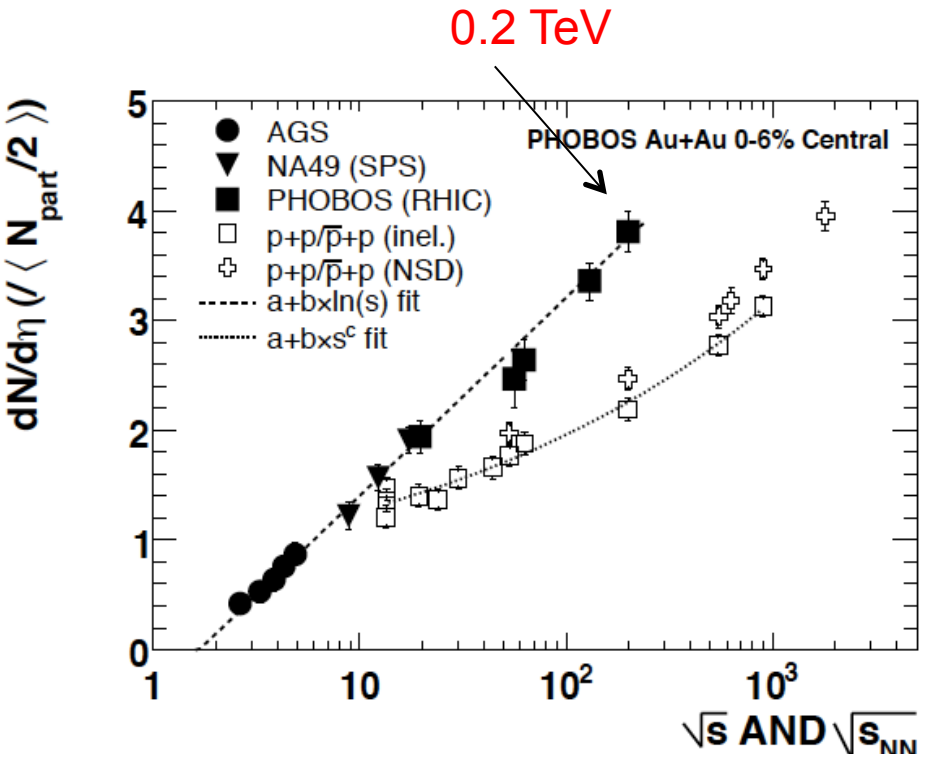

FIG. 3. $dN_{\rm ch}/d\eta|_{|\eta|<1}/\langle N_{\rm part}/2\rangle$ shown for Au+Au collisions as a function of energy. The PHOBOS data, averaged over all available measurement techniques, is compared with lower-energy $A + A$ data as well as a variety of $p + p$ and $\overline{p} + p$ data. The thick dashed line is a fit ($a + b\ln(s)$, with $a = -0.40$ and $b = 0.39$) to the $\sqrt{s_{NN}} =$ 19.6, 130, and 200 GeV data points. The inelastic $p + p$ and $\overline{p} + p$ data have been fit by a function $a + bs^c$ (with $a = 0.35$, $b = 0.52$ and $c = 0.12$), shown by a thin dotted line.

B.B. Back et al., Phobos collab., PRC 74, 021901 (2006).

CMS p+p first results @ 0.9, 2.36 and 7 TeV

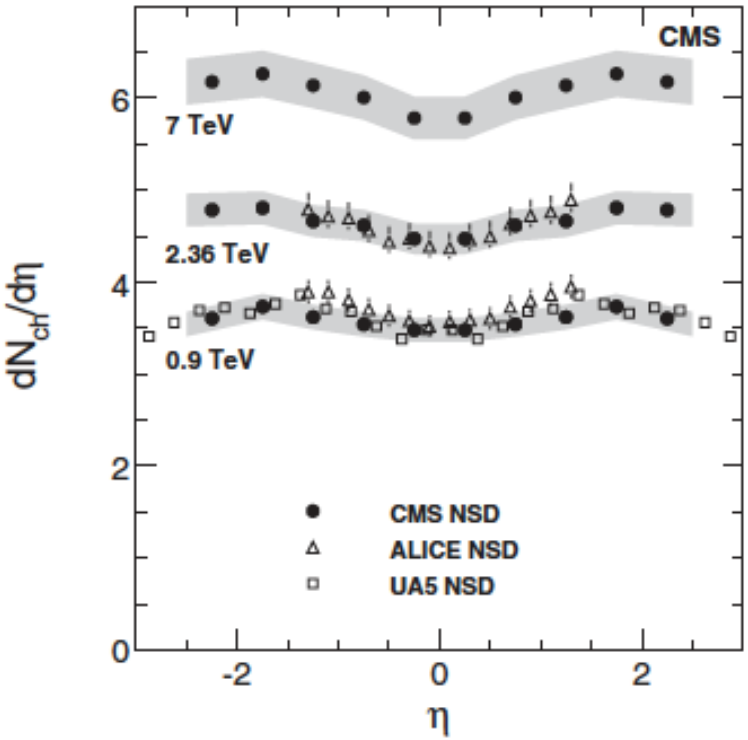

FIG. 3. Distributions of $dN_{ch}/d\eta$, averaged over the three measurement methods and compared with data from UA5 [23] ($p\bar{p}$, with statistical errors only) and ALICE [24] (with systematic uncertainties). The shaded band shows systematic uncertainties of the CMS data. The CMS and UA5 data are averaged over negative and positive values of η.

Pseudorapidity distribution of produced charged hadrons

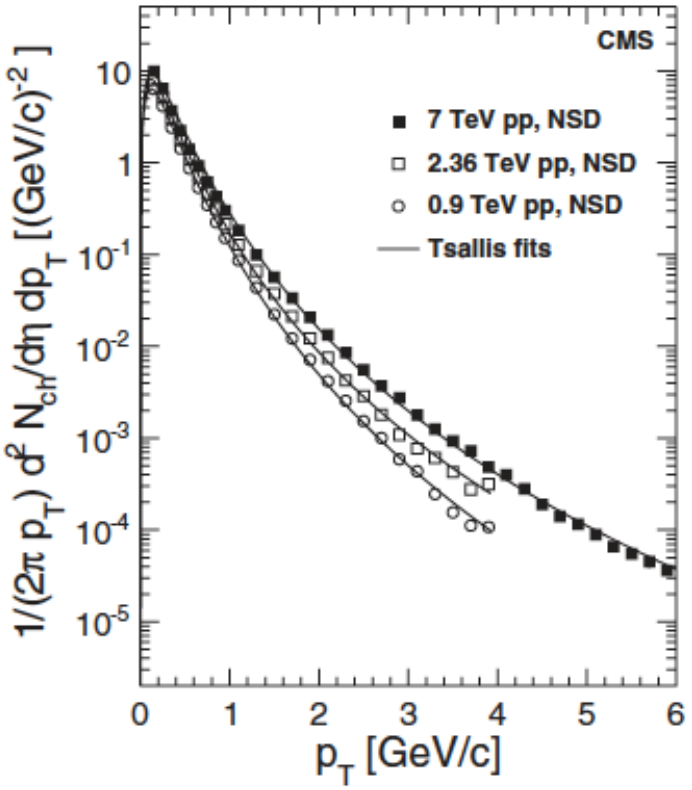

FIG. 2. Charged-hadron yield in the range $|\eta| < 2.4$ in NSD events as a function of p_T; the systematic uncertainties are smaller than the symbols. The measurements at $\sqrt{s} = 0.9$ and 2.36 TeV [3] are also shown. The solid lines represent fits of Eq. (1) to the data.

Transverse momentum distribution of produced charged hadrons

CMS collab., PRL 105, 022002 (2010)

Produced charged hadrons at LHC in a nonequilibrium-statistical model (RDM)

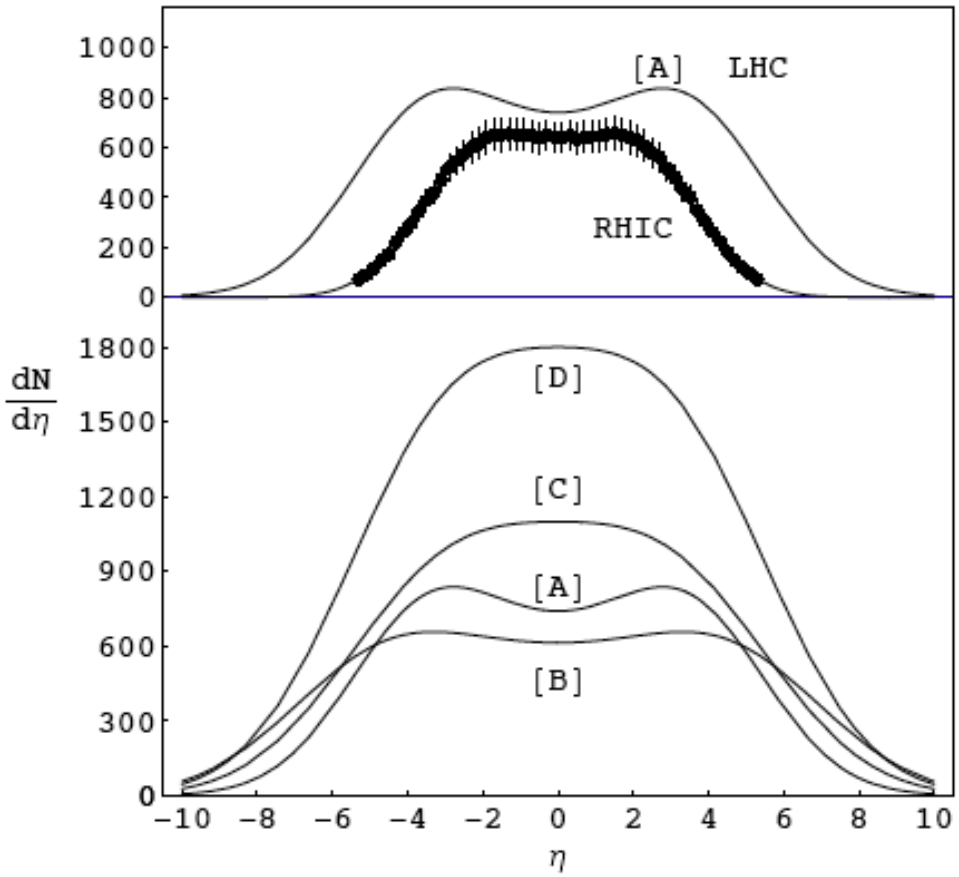

R. Kuiper and G.Wolschin, Annalen Phys. 16, 67 (2006)

LHC: Pb+Pb @ 5.52 TeV
central collisions,
0-6%
[A]: RDM-extrapolation
(sinh-form for τ_{int}/τ_y)
[B]: RDM-extrapolation
(exp-form for τ_{int}/τ_y)
[C]: log-extrapolation
of dn/dη at η=0
[D]: saturation-model (*)
extrap.of dn/dη at η=0

(*) K. Golec-Biernat and M. Wüsthoff, Phys. Rev. D 59, 014017 (1998); N. Armesto et al., PRL 94, 022002 (2005)

LHC dN/dη Predictions

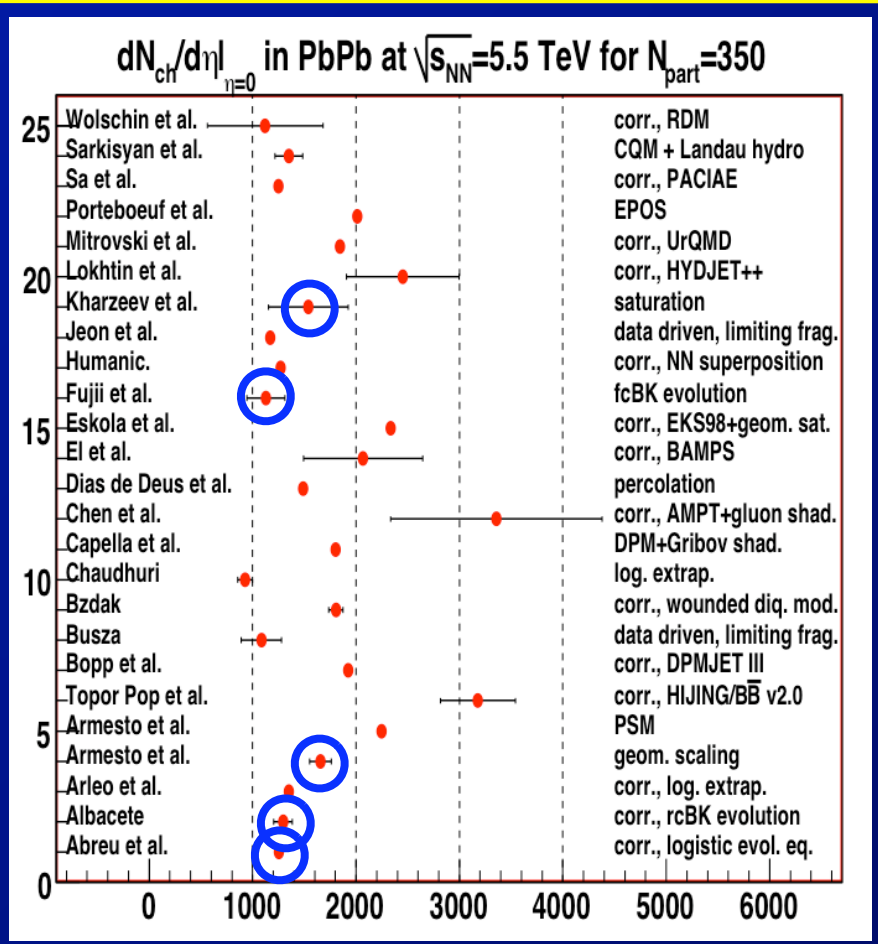

- Many different predictions for LHC Pb+Pb central dN/dη
  - @ 5.5 TeV
- Saturation (motivated) predictions at low end of range
  - 1200-1600

From: B. Cole, ICHEP Paris 2010, and N. Armesto et al., J.Phys. G35, 05400 (2008).

Heavy relativistic systems: Net protons in the Relativistic Diffusion Model

Net-p: (p – $\overline{p}$)

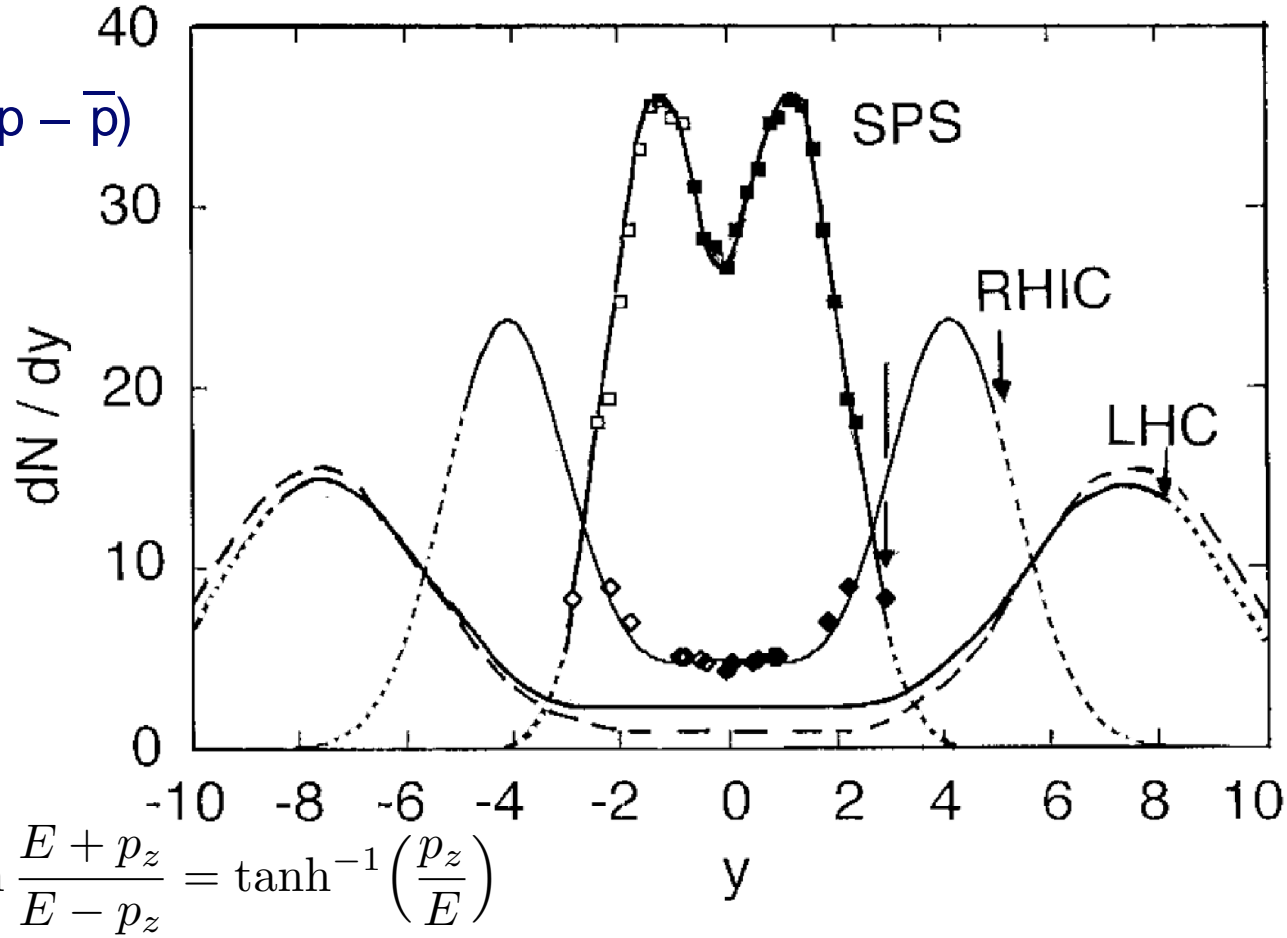

$$y = \frac{1}{2}\ln\frac{E+p_z}{E-p_z} = \tanh^{-1}\left(\frac{p_z}{E}\right)$$

Excess of protons over antiprotons at midrapidity due to baryon-number transfer from the incoming beam

G. Wolschin, Prog. Part. Nucl. Phys. 59, 374 (2007): Nonequilibrium-statistical model (RDM)

Relativistic heavy-ion collisions (Au+Au, Pb+Pb) and gluon saturation

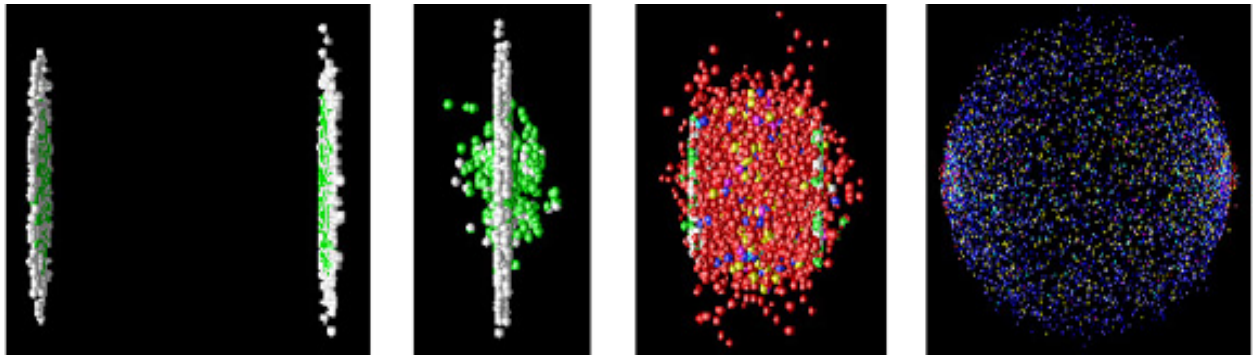

Artwork: UFRA

At RHIC (≤ 0.2 TeV) and LHC (≤ 5.52 TeV) energies, initially a state of very high gluon density (»color glass condensate, CGC«) is formed, which transforms into a strongly coupled quark-gluon plasma (»sQGP«), and then hadronizes after ≈10^{-23} s into mesons and baryons:

Search for signatures of the QGP, and the initial Gluon Condensate in net-baryon and charged-hadron distribution functions.

QCD

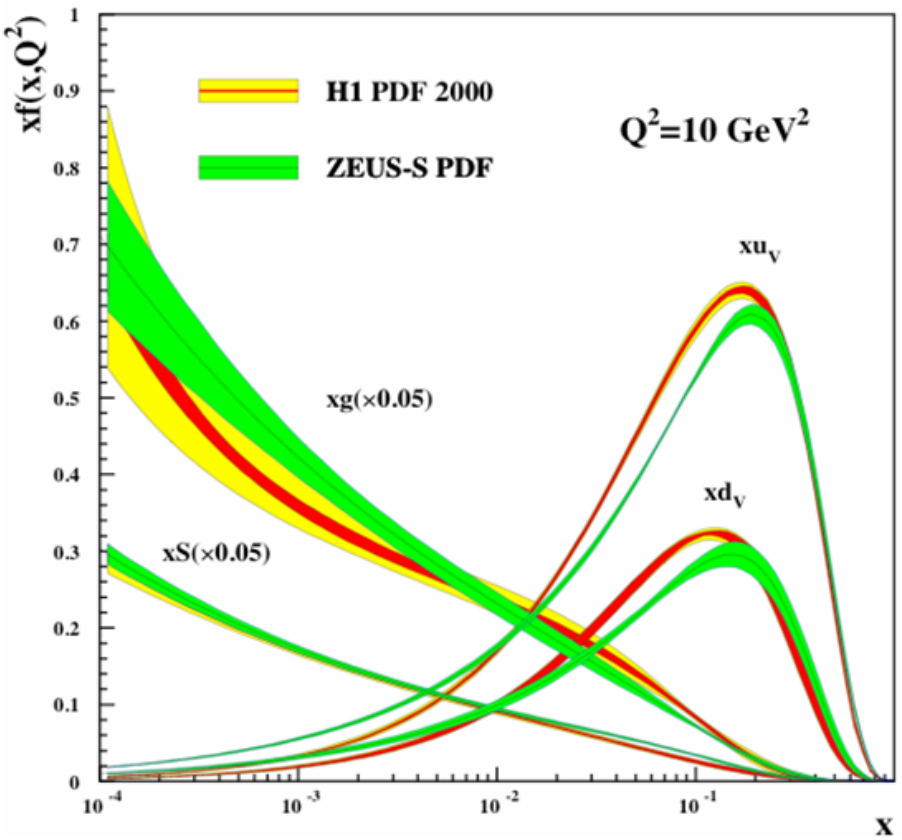

Structure functions (pdfs) from e + p deep inelastic scattering (DIS) at HERA (DESY)

- The parton distribution, ***xf(x,Q^2),*** is the probability density of finding a parton of longitudinal momentum fraction ***x*** and momentum transfer ***Q^2*** in a hadron. In deep inelastic scattering, ***x=Q²/s***.
- At *small x* and high energy, gluons dominate the dynamics.
- The gluon distribution should saturate at very small x.

Geometric scaling

at HERA: e + p collisions

- DIS cross-section is a function of the scaling variable

$$\tau = Q^2/Q_s^2(x)$$

Saturation scale from the data

$$Q_s^2(x) \sim x^{-\lambda} \qquad \lambda \sim 0.3$$

consistent with theoretical results.

Saturation effects scale with $A^{1/3}$ and hence, should be more pronounced in nuclei and in particular, in relativistic heavy-ion collisions.

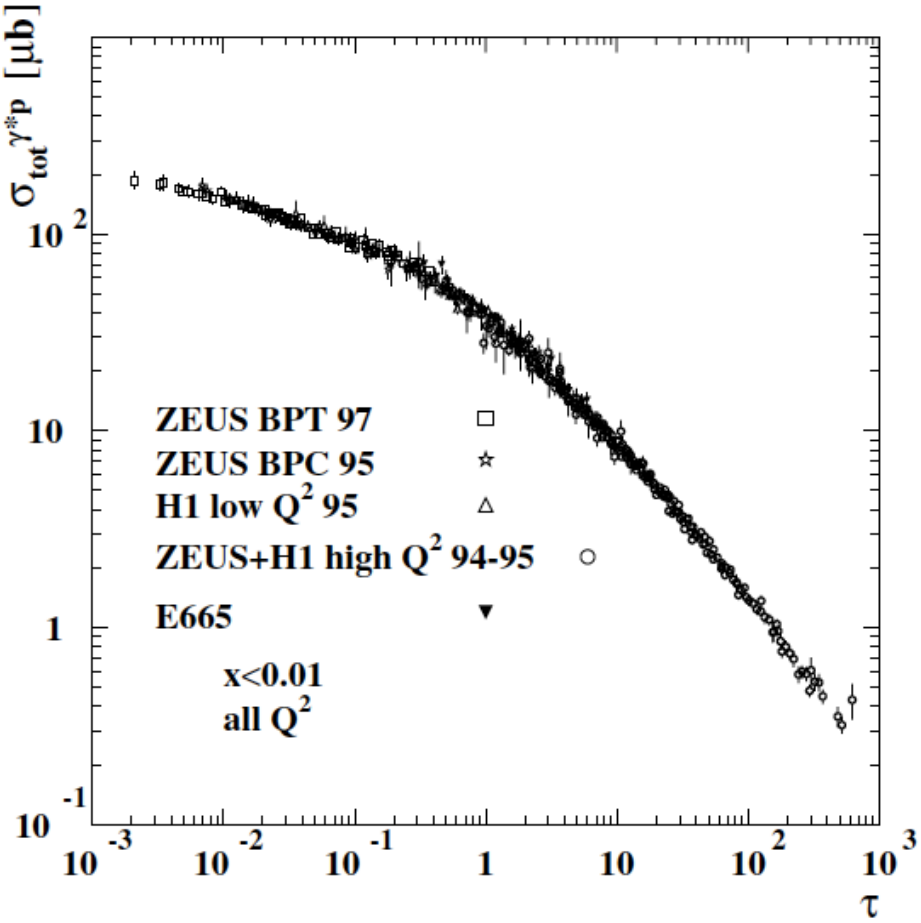

FIG. 1. Experimental data on $\sigma_{\gamma^* p}$ from the region $x < 0.01$ plotted versus the scaling variable $\tau = Q^2 R_0^2(x)$.

Stasto, Golec-Biernat, Kwiecinski, PRL 86, 596 (2001)

2. Microscopic formulation of baryon transport for RHIC, LHC physics

Y. Mehtar-Tani and GW, Phys. Rev. Lett. 102,182301 (2009)

and Phys. Rev. C80, 054905 (2009).

- The net-baryon transport occurs through valence quarks:
- Fast valence quarks in one nucleus scatter in the other nucleus by exchanging soft gluons, and are redistributed in rapidity space.
- The valence quark parton distribution is well known at large x, which corresponds to the forward (and backward) rapidity region, and it can be used to access the small-x gluon distribution in the target.

The differential cross-section for valence quark production with rapidity y and transverse momentum p_T in a high-energy heavy-ion collision is

$$\frac{dN}{d^2p_T dy} = \frac{1}{(2\pi)^2}\frac{1}{p_T^2}\, x_1 q_v(x_1, Q_f)\, \varphi\,(x_2, p_T)$$

The contribution of the valence quarks in the forward moving nucleus to the rapidity distribution of hadrons is then (integration over p_T):

$$\frac{dN}{dy} = \frac{C}{(2\pi)^2}\int \frac{d^2p_T}{p_T^2}\, x_1 q_v(x_1, Q_f)\, \varphi\,(x_2, p_T)$$

Valence quarks

Gluons

Where the transverse momentum transfer is p_T,

the longitudinal momentum fraction carried by the valence quark is $x_1 = p_T/\sqrt{s}\exp(y)$

and the soft gluon in the target carries $x_2 = p_T/\sqrt{s}\exp(-y)$.

Relativistic heavy-ion collisions

As in deep inelastic scattering, geometric scaling is expected:

The gluon distribution depends on x and p_T only through the scaling variable $p_T^2/Q_s^2(x)$ with the saturation scale

$$Q_s^2(x) = A^{1/3} Q_0^2 x^{-\lambda}$$

where $\lambda \approx 0.1$ - 0.3 (fit value in DIS at HERA is $\lambda \approx 0.3$ in agreement with next-to-leading order BFKL results of $\lambda = 0.288$).

Test this in comparison with SPS and RHIC data

Perform a change of variables

$$x \equiv x_1, \quad x_2 \equiv x\, e^{-2y}, \quad p_T^2 \equiv x^2 s\, e^{-2y}$$

then the rapidity distribution can be written as a function of a single scaling variable τ

$$\tau = \ln(s/Q_0^2) - \ln A^{1/3} - 2(1+\lambda)y$$

$$\frac{dN}{dy}(\tau) = \frac{C}{2\pi} \int_0^1 \frac{dx}{x}\, x q_v(x)\, \varphi(x^{2+\lambda} e^{\tau}).$$

For sufficiently large values of x, or the corresponding rapidity, the net-baryon rapidity distribution is a function of a **single** variable that relates the energy (s) dependence to the rapidity (y) and mass number (A) dependence.

There are 3 parameters: C, λ, Q_0.

3. Net-baryon transverse momentum distributions at RHIC energies

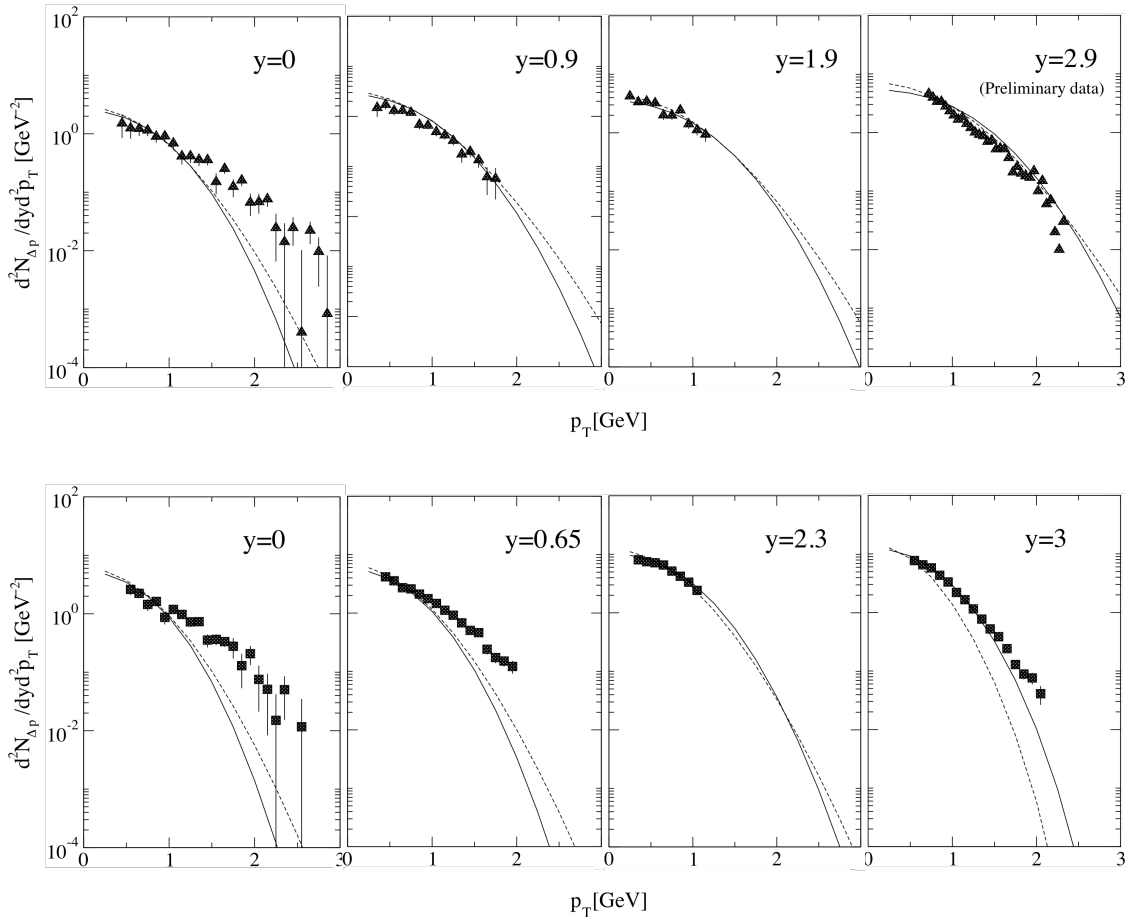

200 GeV (top) and 62.4 GeV (bottom) Au+Au (RHIC) at various rapidities in comparison with BRAHMS data.

Solid curves: Q_0^2 = 0.04 GeV^2, λ=0.2, without fragmentation functions.

Dashed curves: With fragmentation function, Q_0^2 = 0.1 GeV^2.

The saturation scale is

$$Q_s^2(x) = A^{1/3} Q_0^2 x^{-\lambda}$$

Y. Mehtar-Tani and GW, Phys. Rev. C80, 054905 (2009)

4. Net-baryon rapidity distributions at SPS, RHIC, and LHC

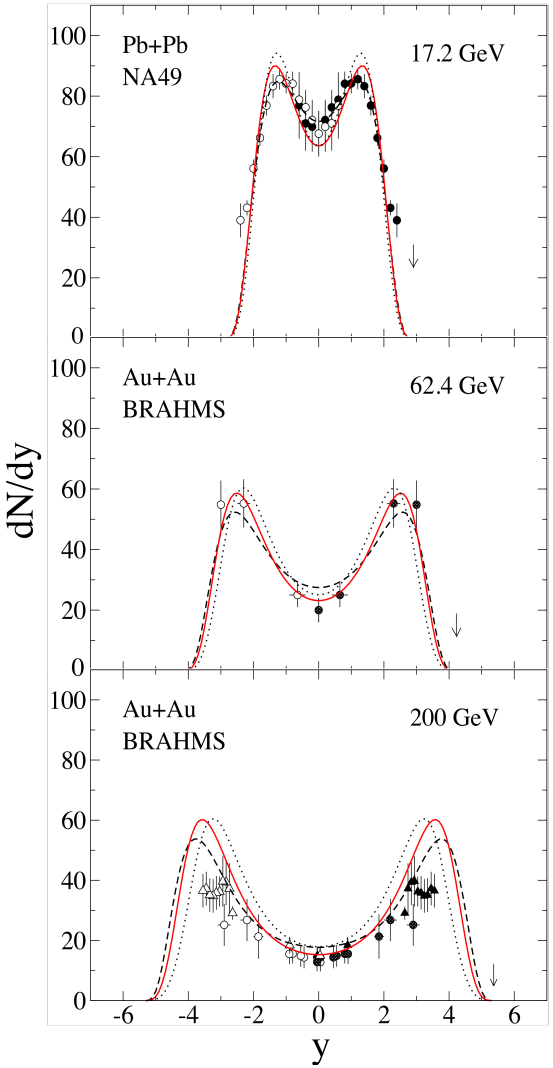

- Central (0-5%) Pb+Pb (SPS) and Au+Au (RHIC) Collisions

- Dashed black curves: Q_0^2 = 0.08 GeV^2 , λ=0
  Solid red curves: Q_0^2 = 0.07 GeV^2, λ=0.15
  Dotted black curves: Q_0^2 = 0.06 GeV^2, λ=0.3

- A larger gluon saturation scale produces more baryon stopping, as does a larger value of A.

- The saturation scale is $Q_s^2(x) = A^{1/3} Q_0^2 x^{-\lambda}$

Y. Mehtar-Tani and GW, Phys. Rev. Lett. 102,182301 (2009).

Net-baryon rapidity distributions at LHC: prediction

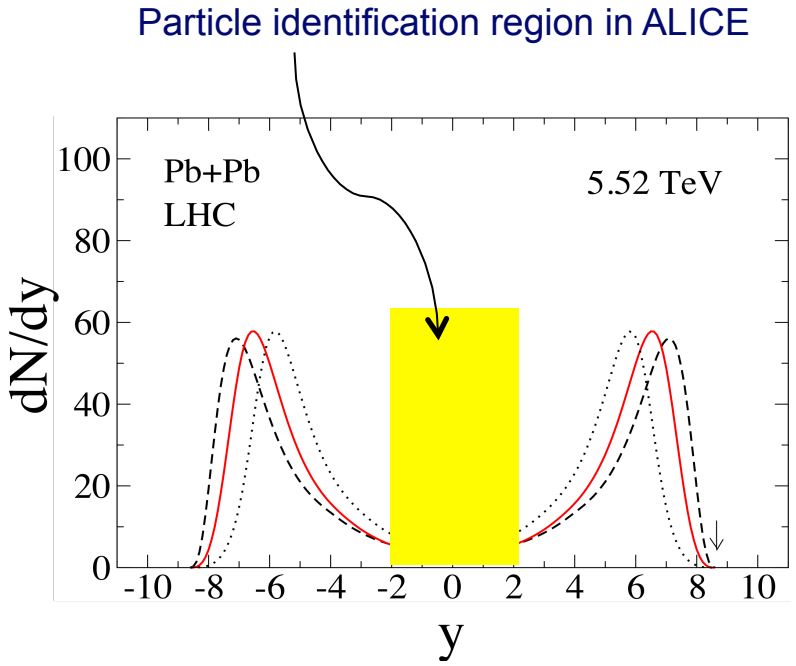

Y. Mehtar-Tani and GW
Phys. Rev. Lett. 102,182301 (2009)

- Central (0-5%) Pb+Pb collisions, $y_{beam} = 8.68$
- Dashed black curve: $\lambda = 0$
  Solid red curve: $\lambda = 0.15$
  Dotted black curve: $\lambda = 0.3$
- A larger gluon saturation scale produces more baryon stopping at LHC as well.
- The midrapidity value of the net-baryon distribution is small, but finite: dN/dy (y = 0) ≈ 4. The **total yield** is normalized to the number of baryon participants, $N_B \approx 357$.

Net-proton rapidity distributions at RHIC and LHC

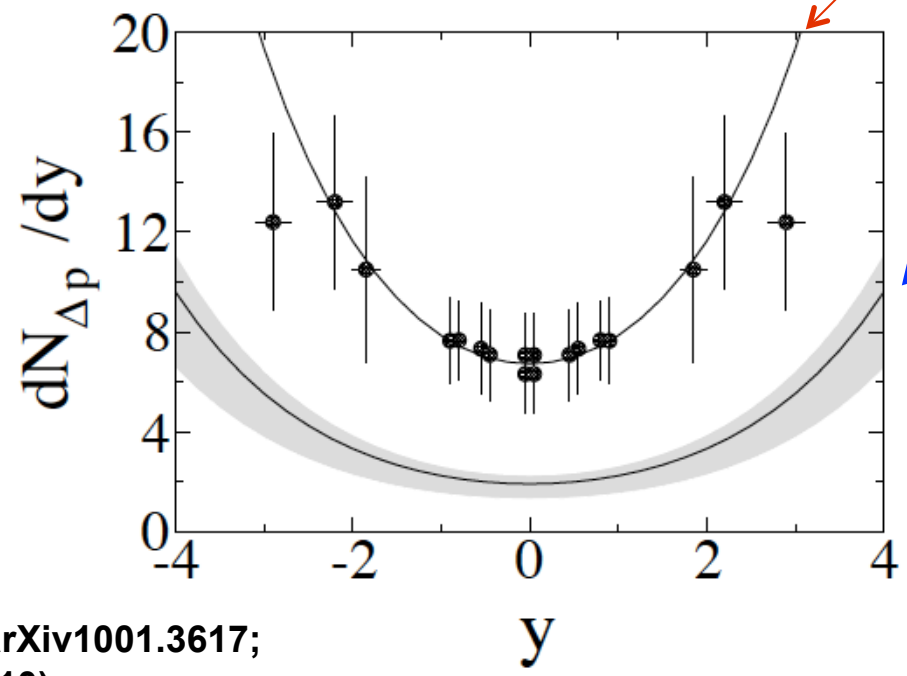

Y. Mehtar-Tani and GW, arXiv1001.3617;
Phys. Lett. B688, 174 (2010)

Figure 1: The rapidity distribution of net protons in central (0%–5%) Au + Au collisions at RHIC energies of $\sqrt{s_{NN}} = 0.2$ TeV as measured by BRAHMS [12] (black dots) is fitted with our theoretical formula using a χ^2- minimization to fix the parameters for the predictions at LHC energies. The data point at y = 2.9 is neglected in the minimization. The grey band in the lower part of the figure shows our predictions for central Pb + Pb collisions at LHC energy of $\sqrt{s_{NN}} = 2.76$ TeV (corresponding to 7 TeV in p + p) with $\lambda = 0.3$ (upper bound), $\lambda = 0.2$ (solid curve), and $\lambda = 0$ (lower bound), using Eq. (6).

Net-proton rapidity distributions at RHIC and LHC

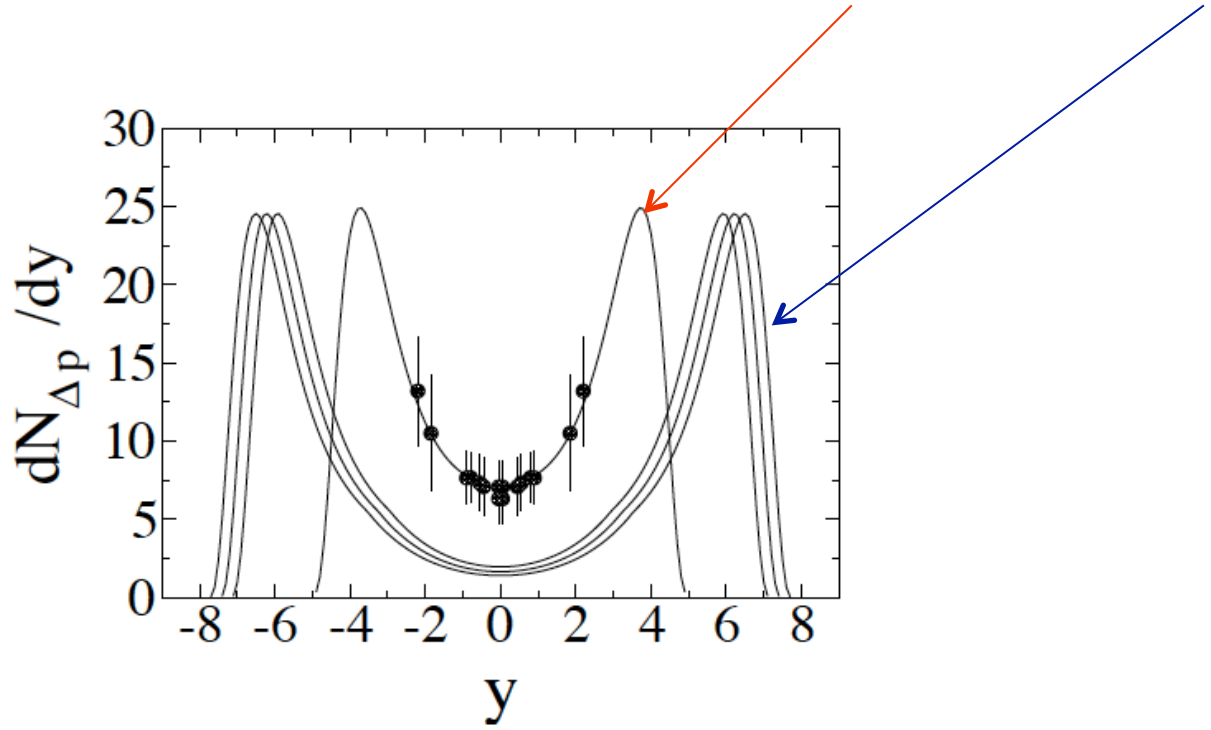

Figure 4: Calculated rapidity distributions of net protons in 0%–5% central Pb + Pb collisions at LHC energies of $\sqrt{s_{NN}} = 2.76, 3.94, 5.52$ TeV. Our result for central Au + Au collisions at RHIC energies of 0.2 TeV is compared with BRAHMS data [12] in a χ^2- minimization as in Fig. 1.

Y. Mehtar-Tani and G. Wolschin, Phys. Lett. B688, 174 (2010)

Mean rapidity loss: from AGS to LHC

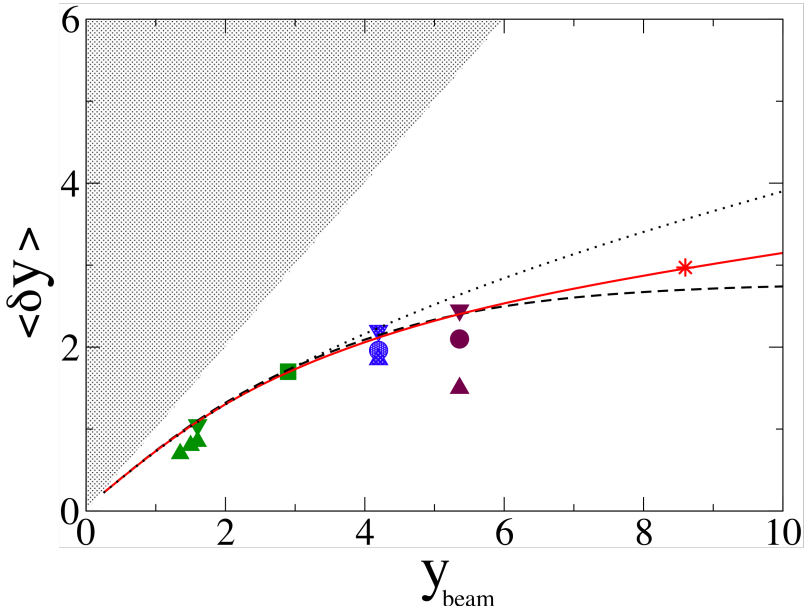

Dotted black curve: λ=0.3
Solid red curve: λ=0.2
Dashed black curve: λ=0
(no x-dependence: the mean rapidity loss reaches a limit at large beam rapidities)

red star: theoretical prediction for LHC

Hence, the value of λ could be determined in heavy-ion collisions at large energies (beam rapidities) above RHIC energies from the mean rapidity loss, or the peak position.

62.4 GeV and 200 GeV RHIC data are from BRAHMS, Phys. Lett. B 677, 267 (2009). 17.3 GeV SPS data are from NA49, low-energy data from AGS.

Y. Mehtar-Tani and G.Wolschin, Phys. Rev. Lett. 102,182301 (2009).

5. Conclusion

- In a QCD-based microscopic model, we have calculated the net-baryon transverse momentum and rapidity distributions for heavy systems at RHIC and LHC energies. They are determined by a single scaling variable τ that depends on the energy, the mass number and the gluon saturation scale.

- LHC: The model allows (in principle) to determine the saturation scale from data on the mean rapidity loss, or from the position of the fragmentation peaks of net-baryon distributions in future forward-physics experiments.

- **Midrapidity Pb + Pb results at LHC energies have been obtained in the microscopic model, and will be compared to net-proton (and net-kaon) data in 2010/2011.**